Biophysical Chemistry 6 (1977) 279–289

FLUORESCENCE DECAY AND QUANTUM YIELD CHARACTERISTICS OF ACRIDINE ORANGE AND PROFLAVINE BOUND TO DNA

Yukio KUBOTA * and Robert F. STEINER

Department of Chemistry, University of Maryland Baltimore County, Baltimore, Maryland 21228, USA

Received 17 November 1976

Fluorescence properties (quantum yield, decay curve, lifetime and polarization) of acridine orange and proflavine bound to DNA were examined as a function of nucleotide to dye (P/D) ratio. First, mean fluorescence lifetimes were determined by the phase-shift measurements. The lifetime and quantum yield of acridine orange increased in a parallel fashion with increasing P/D ratio. There was no parallel relation between the lifetime and quantum yield for proflavine; the lifetime showed a minimum around P/D = 10. Next, fluorescence decay curves were measured by the monophoton counting technique and analyzed with the aid of the method of moments and the Laplace transform method. The results showed that the fluorescence decay of bound acridine orange was exponential above P/D = 10. On the other hand, the decay of bound proflavine was exponential above P/D = 100, but markedly deviated from exponentiality with decreasing P/D ratio. The results of fluorescence polarization suggested that this phenomenon is the result of Förster energy transfer between proflavine molecules bound to the fluorescent site (AT pair) and bound to the quenching site (GC pair). Critical transfer distances were 26.4 and 37.0 A, respectively, for bound proflavine and acridine orange.

1. Introduction

The interaction of fluorescent dyes with DNA is of special interest because of the biological and physicochemical aspects of both the process of small-molecule binding to DNA and the process of charge transfer or energy transfer within the nucleic acid (for review see refs. [1–3]). Fluorescence studies showed that the fluorescence properties of acridine dyes bound to DNA depend on both the dye structure and the nature of the binding sites and that acridine dyes are classified into three types with respect to fluorescence properties; typical results are those of acridine orange (AO), proflavine (PF) and 9-aminoacridine (9-A) [4–7]. If PF is intercalated between adjacent AT pairs, it emits fluorescence of which the quantum yield is nearly equal to that of free dye; however, the presence of only one GC pair in the vicinity of bound PF leads to an almost complete quenching of the fluorescence [5,6,8–11]. It has been also described that acriflavine (10-methylated PF) [12,13] and quinacrine [14–17] behave similarly to PF. There is only one type of site in the case of AO since no quenching of fluorescence can be detected [4–6,18]. Further, the fluorescence quantum yield of 9-A is almost zero when bound to calf thymus DNA [5], suggesting that both AT and GC pairs may be quenching sites. This phenomenon probably is the result of a specific interaction between dyes and binding sites. It is possible that similar interaction may play an important role in the biological actions of acridine dyes [6,19,20].

In an attempt to elucidate the specific interaction between these acridine dyes and binding sites, the fluorescence properties of the dye–nucleotide [21] and dye–DNA systems have been systematically investigated under various conditions. This paper describes the fluorescence lifetime and quantum yield characteristics of AO and PF when bound to DNA, poly d(A–T) and poly (dG) · poly (dC) as a function of P/D. We also report that the fluorescence decay of AO bound to DNA is exponential above P/D = 10, whereas that of PF deviates from exponentiality with decreasing P/D ratio, resulting from Förster energy transfer [22–25] between PF molecules bound to the fluorescent site

* Present address: Department of Chemistry, Yamaguchi University, Yamaguchi 753, Japan.

(AT pair) and bound to the quenching site (GC pair). The results of 9-A have been described elsewhere [26].

2. Materials and methods

2.1. Materials

Calf thymus DNA was purchased from Worthington Biochemical Corporation. Poly d(A—T) and poly (dG) · poly (dC) were obtained from Miles Laboratories. The concentrations of the polynucleotides were calculated from their absorption spectra using the molar extinction coefficients per nucleotide residue [27,28]. The thermal denaturation of DNA was performed by heating the DNA solution for 20 min in boiling water and by then rapidly cooling it in ice water.

AO (Chroma) and PF (British Drug Houses) were purified by repeated crystallization and chromatography. Any trace of impurity was not detected by thin-layer chromatography on silica gel for each dye.

All solutions were made up in 5 mM phosphate buffer (ionic strength of 0.01) at pH 6.9. Low ionic strength was used to minimize the amounts of unbound dye molecules.

2.2. Absorption spectra

Absorbances were measured with a Shimadzu QV-50 spectrophotometer using the expanded scale whenever necessary. Complete absorption spectra were recorded with a Shimadzu UV-200S spectrophotometer.

2.3. Fluorescence spectra and fluorescence polarization

The fluorescence spectra were measured with a Hitachi MPF-2A fluorescence spectrophotometer; they were corrected for the spectral sensitivity of an optical system consisting of lenses, a monochromator and an R446-UR photomultiplier (Hamamatsu TV). Slitwidth was used for assuring a resolution of 2 nm.

Fluorescence quantum yields were determined according to the method described by Parker and Rees [29]. First, to determine the quantum yields of AO and PF the area under the corrected fluorescence spectrum plotted against wavenumber was compared with the corresponding area obtained with the fluorescence standard. Quinine sulfate was used for the standard [30,31]. Next, the quantum yield of the complex at a given P/D was determined by comparing the area under the corrected fluorescence spectrum of the complex with that of free dye. It is necessary to consider the artifacts due to the polarization when measuring the quantum yields; various methods to avoid such artifacts have been suggested [32—35]. In this study we generally used the following procedure [18]. A total intensity of fluorescence at a given wavelength (I_F) is obtained by:

$$I_F = I_{VV} + 2I_{VH}\, I_{HV}/I_{HH}, \tag{1}$$

where I_{VV}, I_{VH}, I_{HH} and I_{HV} are the intensities of the four components of the fluorescent light. The subscripts denote the directions of polarization; the first letter for the exciting light and the second for the fluorescence. The factor, I_{HV}/I_{HH}, corrects for the unequal transmitivity of the emission monochromator for light polarized horizontally or vertically [36]. To avoid a troublesome correction of the measurements at all wavelengths, a correction curve was established for each system as a function of P/D. This curve gives the ratio of the total intensity measured at maximum wavelength to the total area of the corrected fluorescence spectrum.

Polarization of fluorescence was measured with the same fluorescence spectrophotometer, with a pair of Polacoat dichroic filters as the polarizer and the analyzer. With the incident beam vertically polarized, the degree of polarization (P) is given by [36]:

$$P = \frac{I_{VV} - I_{VH}\, I_{HV}/I_{HH}}{I_{VV} + I_{VH}\, I_{HV}/I_{HH}}. \tag{2}$$

2.4. Fluorescence lifetimes and decay curves

Fluorescence lifetimes were measured with a JASCO FL-10 phase fluorometer using exciting light modulated at 13.56 MHz [5]. If the fluorescence response function is $I(t)$, its fluorescence response to an exciting light function $E(t)$ is given by the convolution integral [37]:

$$F(t) = \int_0^\infty E(t-u)I(u)\,du, \tag{3}$$

where $E(t)$ is a periodic function, which may be expressed as a Fourier series in terms of the fundamental angular frequency ω. When θ is a phase difference between $F(t)$ and $E(t)$, one obtaines the following equation:

$$\tan\theta = \int_0^\infty \sin\omega t\, I(t)\mathrm{d}t \Big/ \int_0^\infty \cos\omega t\, I(t)\mathrm{d}t. \qquad (4)$$

In general $I(t)$ is assumed to be a monoexponential or multiexponential function:

$$I(t) = \sum \alpha_i \exp(-t/\tau_i), \qquad (5)$$

where α_i and τ_i are the amplitude and lifetime, respectively, of the ith component. If $I(t)$ is a monoexponential function, eq. (4) leads to:

$$\tan\theta = \omega\tau. \qquad (6)$$

Eq. (6) is the basic equation of the phase fluorometer. Unfortunately, one cannot always assume a homogeneous emitting population. If $I(t)$ is a multiexponential function like eq. (5), the average value of the phase shift is given by:

$$\overline{\tan\theta} = \omega\langle\tau\rangle, \qquad (7)$$

where

$$\langle\tau\rangle = \frac{\Sigma\alpha_i\tau_i^2/(1+\omega^2\tau_i^2)}{\Sigma\alpha_i\tau_i/(1+\omega^2\tau_i^2)}. \qquad (8)$$

Fluorescence decay curves were obtained with an Ortec 9200 monophoton counting nanosecond fluorometer. Appropriate Corning filters and Baird Atomic interference filters were used to select the excitation and emission wavelengths. A correction was made for the contribution of the scattered light and emission from the interference filter by subtraction of the appropriate controls. In this technique the exciting light function $E(t)$ is a recurrent light pulse of short duration. Then the observed emission $F(t)$ is given by the convolution [37]:

$$F(t) = \int_0^t E(t-u)I(u)\mathrm{d}u. \qquad (9)$$

Deconvolution of eq. (9) to obtain $I(t)$ was done with the aid of both the method of moments [38,39] and the Laplace transform method [40], assuming that $I(t)$ is expressed by eq. (5). Copies of these computer programs are kindly supplied to us by Dr. R.D. Dyson and Dr. L. Brand. On the other hand, in the cases of energy transfer [22–24,41,42] and fluorescence quenching [43], the decay law actually follows:

$$I(t) = I_0 \exp[-(at + bt^{1/2})]. \qquad (10)$$

In this case, we generally used the following procedure. Assuming appropriate values of a and b in eq. (10), we tried several $I(t)$ functions so that the numerically computed convolution with the profile of the exciting light pulse may fit the experimental curve. The computed curve, $F^0(k)$, was then visually compared with the experimental curve, $F(k)$, and the weighed residue (χ^2) was calculated according to the method of Knight and Selinger [44]:

$$\chi^2 = \frac{1}{n}\sum_{k=1}^{n}\frac{[F(k)-F^0(k)]^2}{F(k)}. \qquad (11)$$

The quality of the fits was judged from two standpoints: (1) the overlap between the experimental decay curve and the computed decay curve and (2) the smallest χ^2 value. A Univac 1108 computer was used for all analyses.

The natural decay of fluorescence, $I_\parallel(t) + 2I_\perp(t)$, was obtained by two methods [45,46]: (1) The emission is observed without the polarizer by orienting the analyzer at an angle of 35.3° to the normal axis of the experimental plane and (2) the emission is observed by orienting the analyzer at an angle of 54.7° to the normal axis using the exciting light vertically polarized. Both methods gave the same decay curves.

For all measurements, the temperature was 23 ± 1°C unless otherwise stated.

3. Results and discussion

3.1. Fluorescence lifetimes and quantum yields of AO and PF bound to DNA

If we examine the fluorescence of a constant concentration of AO and PF over a wide range of P/D, the results shown in figs. 1 and 2 are obtained. Here mean fluorescence lifetimes ($\langle\tau\rangle$) were obtained from the phase-shift measurements. The quantum yield

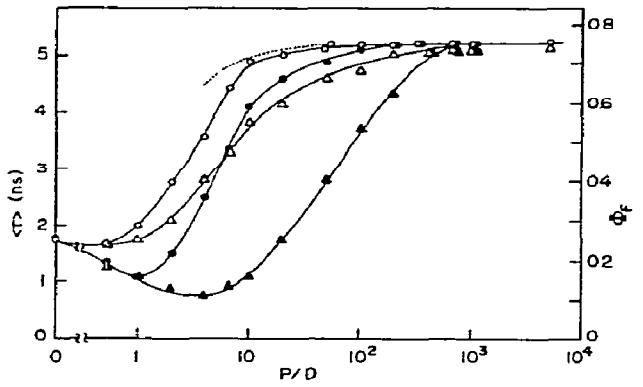

Fig. 1. Mean fluorescence lifetimes ($\langle\tau\rangle$) and quantum yields (Φ_F) of AO bound to DNA as a function of P/D. The solvent was 5 mM phosphate buffer (pH 6.9) at 23°C. The dye concentration was 2.0×10^{-6} M. The excitation wavelength was 450 nm. τ: ○ native DNA, △ denatured DNA. Φ_F: ● native DNA, ▲ denatured DNA. The dotted curve shows the mean lifetimes ($\langle\tau\rangle$) computed on the assumption that the fluorescence results from both free and bound dye molecules (see text for details).

profile of AO is in agreement with previous findings [4,18,47,48]. As is seen in fig. 1, the lifetime and quantum yield of AO bound to native DNA increase in a parallel fashion with increasing P/D ratio. On the other hand, the lifetime of PF bound to native DNA decreases with decreasing P/D ratio and shows a minimum around P/D = 10; there is no parallel relation between the lifetime and the quantum yield (fig. 2).

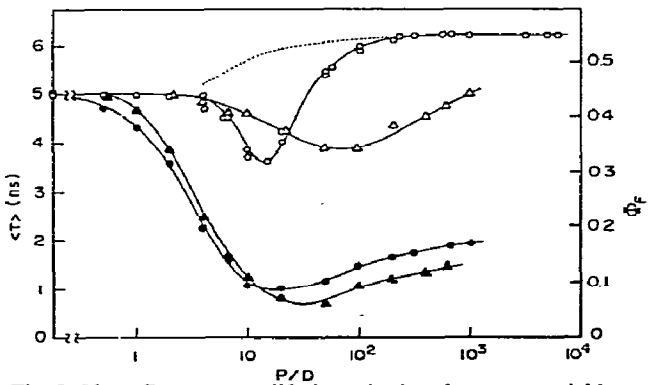

Fig. 2. Mean fluorescence lifetimes ($\langle\tau\rangle$) and quantum yields (Φ_F) of PF bound to DNA as a function of P/D. The dye concentration was 2.0×10^{-6} M. The excitation wavelength was 400 nm. The symbols and the dotted curve are the same as for fig. 1.

It should be noted that the observed yield and the lifetime calculated from the phase-shift measurements were average values which must be considered dependent on the number of fluorescence components present in solution [49,50]. The decay-curve measurements by the monophoton counting technique revealed that the fluorescence decays of AO and PF are monoexponential at a high P/D ratio; this will be described later. For the sake of simplicity, we first assume that the emission at a lower P/D ratio results from both free and bound dye molecules. Then the fluorescence response function $I(t)$ is given by:

$$I(t) = \alpha_1 \exp(-t/\tau_f) + \alpha_2 \exp(-t/\tau_b), \qquad (12)$$

where

$$\alpha_1 = \epsilon_f C_f \Phi_f / (\epsilon_f C_f + \epsilon_b C_b),$$
$$\alpha_2 = \epsilon_b C_b \Phi_b / (\epsilon_f C_f + \epsilon_b C_b) \qquad (13)$$

and where ϵ is the molar extinction coefficient at excitation wavelength, C the concentration of dye and Φ the quantum yield of fluorescence; the subscripts f and b denote free and bound dye molecules. The values of C_f and C_b were calculated on the basis of equilibrium dialysis [51]. Then the mean lifetimes ($\langle\tau\rangle$) were computed according to eqs. (12), (13) and (8); the results are shown by dotted lines in figs. 1 and 2. The calculated curve roughly coincides with the observed curve above P/D = 10 for DNA–AO system (fig. 1). From the data of equilibrium dialysis and spectroscopy, Armstrong et al. [52] suggested that, at low ionic strength, a binding of dye dimers takes place at low P/D ratios by binding of a second dye molecule to those already intercalated. Fredericq and Houssier [18] could show that a continuous decrease of fluorescence with decreasing P/D ratio is reasonably explained if we admit that such bound dimers do not fluoresce at all. Thus an agreement between the calculated and observed curves for $\langle\tau\rangle$ is expected by substituting an appropriate mole fraction of bound dimers into eq. (13).

The fluorescence is remarkably quenched around P/D = 1; this probably originates from the external binding of highly aggregated molecules [18,53,54]. On the other hand, the curve for denatured DNA has a very different trend (fig. 1). A high quantum yield and lifetime are not attained until the P/D ratio becomes sufficiently high. This may be due to the existence of only limited renatured parts of DNA

Table 1
Fluorescence lifetimes and quantum yields of AO and PF bound to poly d(A–T) and poly (dG) · poly (dC). The solvent is 5 mM phosphate buffer (pH 6.9) at 23°C

System [a]	P/D	⟨τ⟩(ns) [b]	Φ_F
AO		1.7	0.25
AO + poly d(A–T)	203	5.4	0.76
	102	5.3	0.75
	51	5.2	0.72
	20	5.3	0.68
	10	5.1	0.60
AO + poly (dG) · poly (dC)	161	5.6	0.78
	101	5.7	0.77
	51	5.7	0.77
	20	5.5	0.69
	10 [c]	4.7	0.57
PF		5.0	0.44
PF + poly d(A–T)	202	7.0_5	0.52
	101	7.1 (7.1)	0.52
	50	7.0_5	0.52
	20	6.9_5	0.51
	10	6.9 (6.8)	0.50
PF + poly (dG) · poly (dC)	202	1.3_5	0.01_5
	101	1.4_5	0.01_5
	50	1.7_5	0.02
	20 [c]	3.5	0.03
	10 [c]	4.4	0.06

[a] The concentrations of AO and PF were 2.0×10^{-6} and 2.7×10^{-6} M, respectively.
[b] Determined from the phase-shift measurements; the measurements were made several times, and the results averaged. The values in parentheses were obtained by the monophoton counting technique.
[c] The contribution of free dye was not negligible.

where intercalation can take place; a strong quenching of fluorescence is attributed to the external binding of aggregates [53,54].

In the case of PF, an agreement between the calculated and observed curves for ⟨τ⟩ is not seen (fig. 2). This clearly indicates that the emission of PF when bound to DNA includes one or more shorter components or that the decay law follows an alternative mechanism; this will be discussed later. The lifetime for denatured DNA does not reach the value for native DNA even at high P/D ratios (fig. 2).

The value of $\langle\tau\rangle/\langle\tau\rangle_0$ is equal to that of $\Phi_F/(\Phi_F)_0$ at a high P/D ratio for DNA–AO complexes, whereas this relation does not hold for DNA–PF complexes (figs. 1 and 2); here $\langle\tau\rangle_0$ and $(\Phi_F)_0$ are the lifetime and the quantum yield, respectively, of free dye. This finding offers evidence for at least two types of binding sites for PF and only one type of site for AO [4,5,8].

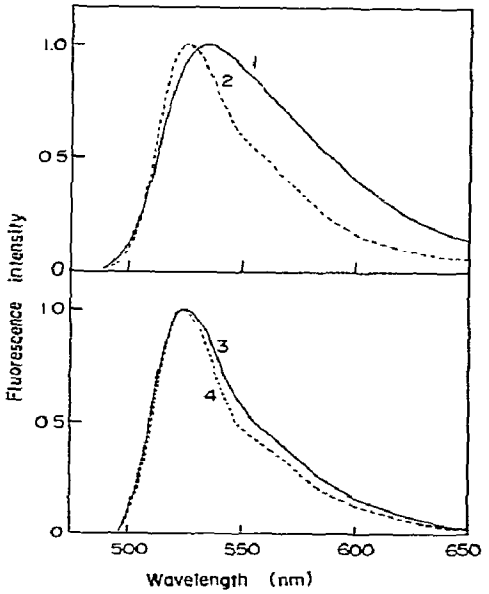

Fig. 3. Normalized corrected fluorescence spectra of AO (2.0×10^{-6} M) in 5 mM phosphate buffer (pH 6.9) at 23°C: (1) free, (2) bound to DNA (P/D = 200), (3) bound to poly d(A–T) (P/D = 203) and (4) bound to poly (dG) · poly (dC) (P/D = 161). The excitation wavelength was 450 nm.

3.2. Fluorescence lifetimes and quantum yields of AO and PF bound to poly d(A–T) and poly (dG) · poly (dC)

To obtain further information on the interaction between acridine dyes and the binding sites, we next examined the fluorescence properties of dyes when bound to poly d(A–T) and poly (dG) · poly (dC) which contain only one type of site. The fluorescence lifetimes and quantum yields are summarized in table 1. They confirm and extend previous observations which were obtained at a high P/D ratio [5,6]. There is a striking parallelism between lifetimes and quantum yields except for the PF–poly (dG) · poly (dC) system; $\langle\tau\rangle/\langle\tau\rangle_0 \approx \Phi_F/(\Phi_F)_0$. When PF is bound to poly (dG) · poly (dC), the fluorescence is remarkably quenched with increasing P/D ratio.

Fluorescence spectra are shown in figs. 3 and 4 by normalizing their maxima to unity; a blue-shift and a narrowing of the fluorescence band are observed when

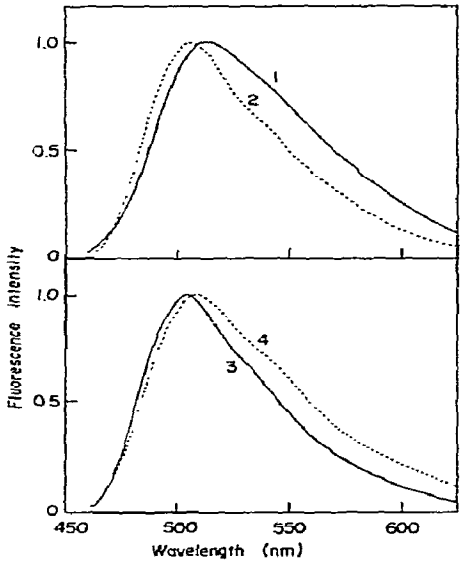

Fig. 4. Normalized corrected fluorescence spectra of PF (2.7×10^{-6} M) in 5 mM phosphate buffer (pH 6.9) at 23°C: (1) free, (2) bound to DNA (P/D = 200), (3) bound to poly d(A–T) (P/D = 202) and (4) bound to poly (dG) · poly (dC) (P/D = 202). The excitation wavelength was 400 nm.

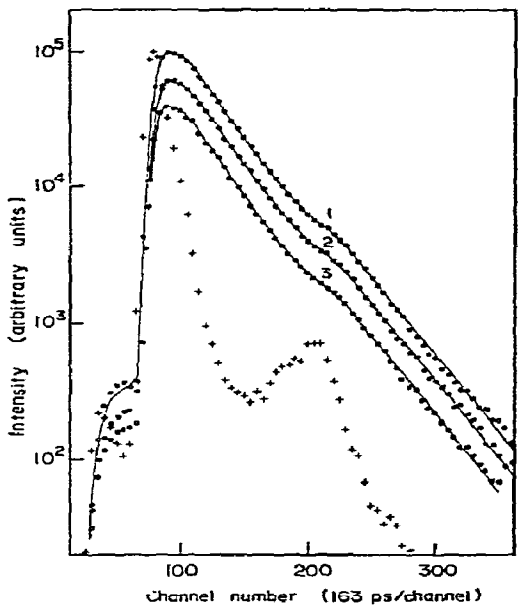

Fig. 5. Fluorescence decay curves of AO (5.0×10^{-6} M) bound to DNA. The solvent was 5 mM phosphate buffer (pH 6.9) at 23°C. Open and solid circles are observed decay curves. Solid lines are calculated on the assumption that the lifetime is 5.5_9 ns for (1) P/D = 202, 5.5_1 ns for (2) P/D = 20 and 5.3_8 ns for (3) P/D = 10. + is the time course of exciting light pulse. The excitation and emission wavelengths were 430 and 525 nm, respectively.

compared to that of free dye [4–6,11,18,55]. It can be seen from figs. 3 and 4 that the fluorescence spectrum of AO bound to DNA is intermediate between those of AO bound to poly d(A–T) and poly (dG) · poly (dC) [55] and that of PF bound to DNA is identical with that of PF bound to poly d(A–T). The results obtained here clearly lead to the following conclusions: Both AT and GC pairs are fluorescent sites for AO, and the AT pair is responsible for the fluorescence of PF, but the GC pair almost completely quenches the fluorescence.

A continuous decrease of the quantum yield is observed with decreasing P/D ratio for AO–polynucleotide systems. It seems likely that this phenomenon is a result of the formation of non-fluorescent dye dimers as well as in the case of DNA–AO complexes [18,52]. The results of PF–poly d(A–T) complexes show that the quantum yield and the lifetime remain almost constant until conditions of incomplete dye binding are reached. This is probably due to a lower tendency of PF to form non-fluorescent bound dimers [52].

3.3. Fluorescence decay curves of AO and PF bound to DNA

Finally, we measured the fluorescence decay curves by the monophoton counting technique to elucidate the decay kinetics. Some typical decay curves of AO bound to DNA are shown in fig. 5. After deconvolution using both the method of moments [38,39] and the Laplace transform method [40], the emission decay was found to be a single exponential above P/D = 10. In general, both methods gave the same lifetimes. The deconvoluted results are listed in table 3 together with the mean lifetimes ($\langle\tau\rangle$) obtained by phase fluorometry. The lifetimes obtained by nanosecond pulse fluorometry are slightly larger than the corresponding $\langle\tau\rangle$ values, but the agreement between both values is satisfactory.

In contrast, the decay curves of PF when bound to DNA showed a marked deviation from exponentiality

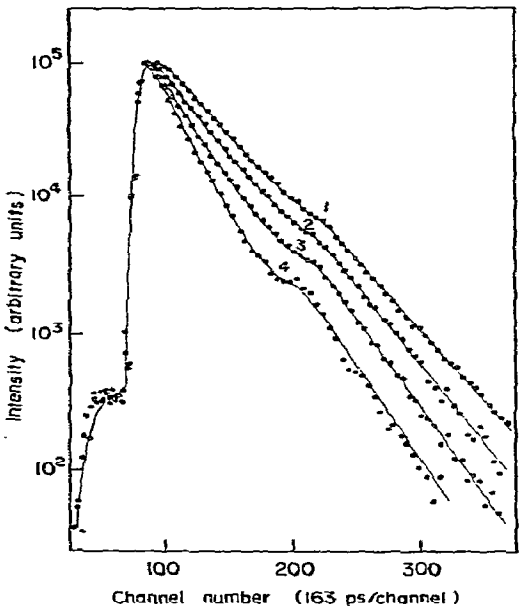

Fig. 6. Fluorescence decay curves of PF (4.8×10^{-6} M) bound to DNA. The solvent was 5 mM phosphate buffer (pH 6.9) at 23°C. Open and solid circles are observed decay curves. Solid lines are attempts to fit to $\exp(-t/\tau)$ for (1) P/D = 214 and to fit to $\exp[-t/\tau - 2q(t/\tau)^{1/2}]$ for (2) P/D = 51, (3) P/D = 20 and (4) P/D = 11. The best fits were obtained when τ and q are the following: (1) $\tau = 6.4_0$ ns, (2) $\tau = 6.4_0$ ns and $q = 0.07$, (3) $\tau = 6.4_0$ ns and $q = 0.40$, (4) $\tau = 6.4_0$ ns and $q = 0.75$. The excitation and emission wavelengths were 430 and 500 nm, respectively.

with decreasing P/D ratio (fig. 6). First the observed decay curves were deconvoluted on the assumption that the decay law obeys a multiexponential function like eq. (5). The deconvoluted results showed that the decay above P/D = 100 is a single exponential (table 3), while the decay below P/D = 100 is a sum of two or three exponentials. For example, the analyses by the method of moments led to the following results:

$$I(t) = 0.68e^{-t/6.1_2} + 0.32e^{-t/1.3_5} \quad \text{at P/D} = 51,$$
$$I(t) = 0.46e^{-t/5.3_1} + 0.54e^{-t/1.1_5} \quad \text{at P/D} = 20.$$

The shorter decay time constants (1.1_5 and 1.3_5 ns) are very close to the value (1.3_5–1.4_5 ns) for PF bound to poly (dG) · poly (dC), and the longer decay constants (5.3_1 and 6.1_2 ns) are close to the value at a high P/D ratio or the value for PF bound to poly d(A–T) (table 1).

If DNA has at least two types of sites and a preferential binding of PF to these sites is possible, the above results might be reasonably understood: PF first occupies the fluorescent site (AT pair) and then the quenching site (GC pair). However, the preferential binding seems unlikely on the basis of the theoretical and experimental results: the former shows that most intercalation sites have almost equal binding affinity [56] and the latter shows that the binding constants of acriflavine and PF are independent of the GC content of DNA [9,10,13]. Furthermore, as judged from the quantum yields of PF when bound to poly d(A–T) and poly (dG) · poly (dC) (table 1), the amplitude of the shorter decay component appears too big in the case of calf thymus DNA (GC content of 42%).

Very recently, Georghiou has claimed that the fluorescence decay of PF when bound to DNA is non-exponential even at a high P/D ratio and the deviation from exponentiality becomes more pronounced as the GC content increases [11]. On the contrary, our analyses of decay curves clearly show that the decay is a single exponential at a high P/D ratio when bound to calf thymus DNA (fig. 6; table 3). In agreement with this, the measurements of fluorescence spectra show that the emission should be attributed to PF bound to AT-rich regions of DNA (fig. 4). Even though there exists any shorter decay component, this would exert only a minor effect on the decay curves in the present DNA (GC content of 42%). The heterogeneity of the emission might appear as the GC content increases further [11,16]. Accordingly, the hypothesis that PF molecules distribute over various quenching sites seems inadequate to explain the dependence of the decay curves on P/D shown in fig. 6.

3.4. Energy transfer between bound dye molecules

Since the absorption spectrum of PF when bound to DNA overlaps its fluorescence spectrum (fig. 7), Förster energy transfer between bound dye molecules is possible. According to the theory of Förster [22–25], the critical transfer distance R_0 where energy transfer is 50% efficient is given by:

$$R_0 \text{ (in Å)} = (9.79 \times 10^3)(J\kappa^2\Phi_D n^{-4})^{1/6}. \qquad (14)$$

where

$$J = \int_0^\infty F(\bar{\nu})\epsilon(\bar{\nu})\bar{\nu}^{-4}\,d\bar{\nu}. \qquad (15)$$

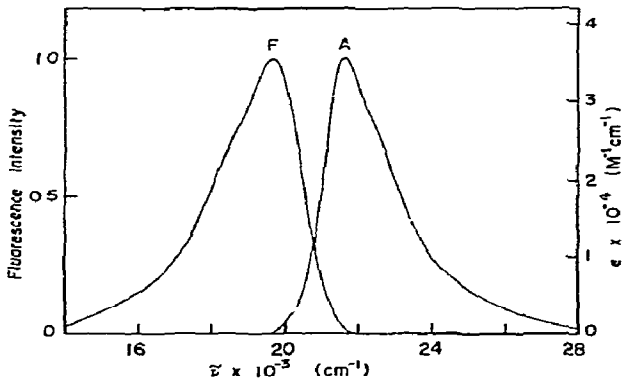

Fig. 7. Absorption (A) and fluorescence (F) spectra of DNA–PF complex at a high P/D value.

Table 2
Critical transfer distance R_0

	DNA–AO	DNA–PF
$J \times 10^{15}$ ($cm^6 M^{-1}$)	38.4	8.43
n [a]	1.6	1.6
Φ_D	0.75	0.45 [b]
R_0 (A)	37.0	26.4

a) Obtained from ref. [60].
b) Fluorescence quantum yield of PF intercalated between adjacent AT pairs. It can be obtained by dividing the apparent quantum yield of PF bound to DNA (0.15) by the mole fraction of adjacent AT pairs (0.3364) on the assumption that PF molecules are randomly distributed [5].

$$\kappa = \cos\theta_{DA} - 3\cos\theta_D \cos\theta_A, \qquad (16)$$

and where Φ_D is the quantum yield of the donor fluorescence in the absence of acceptor, n is the refractive index of the medium, $F(\bar{\nu})$ is the quantum fluorescence spectrum of the donor normalized to 1, $\epsilon(\bar{\nu})$ is the molar extinction coefficient of the acceptor at the wavenumber $\bar{\nu}$, θ_{DA} is the angle between the donor and the acceptor dipoles, θ_D and θ_A are the angles between the donor and the acceptor dipoles, respectively, and the line joining them. With the intercalation model where a dye molecule is sandwiched between adjacent base pairs [57,58], κ^2 takes a simplified value: since $\theta_D = \theta_A = 90°$, $\kappa^2 = \cos^2\theta_{DA}$, showing that κ^2 is between 0 and 1. However, the dipole orientation factor cannot be directly measured. In the calculations that follow a value of $\kappa^2 = \frac{2}{3}$ has been assumed [25]. The value of n was estimated to be 1.4 for RNA [59], but a somewhat higher value ($n = 1.6$) would be predicted for DNA [60]. Finally, R_0 values listed in table 2 are obtained.

Energy transfer between like molecules causes only a depolarization of the emission and is not responsible for descreases in both the lifetime and the quantum yield [22–24,61]. To check this point, the polarization of fluorescence was measured as a function of P/D. In agreement with previous findings [4,18], a streng decrease in the polarization with decreasing P/D ratio is observed in the case of AO (fig. 8). Weill and Calvin [4] calculated that the polarization resulting from energy transfer between intercalated dye molecules should be 0.135 by assuming an equal probability of energy transfer for each transfer distance. It is interesting that this value is very close to our observed value at a low P/D ratio. The exact nature of polarization behavior should depend on the unwinding or winding angle of the DNA helix by the intercalation as has been quantitatively treated by Paoletti and LePecq [62] and Wahl et al. [63] in the case of ethidium bromide binding to DNA. However, the results obtained here provide a satisfactory proof of the occurrence of energy transfer.

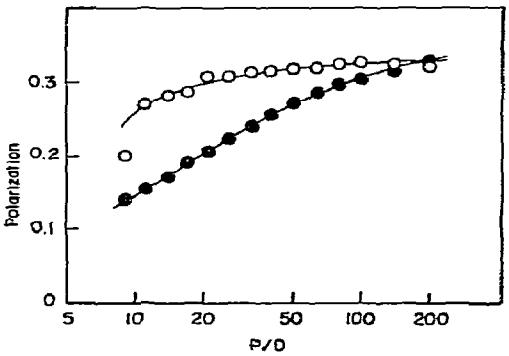

Fig. 8. The degree of polarization of DNA–AO (•) and DNA–PF (o) complexes as a function of P/D. The solvent was 5 mM phosphate buffer (pH 6.9) at 23°C. The intensities of fluorescence were corrected for the contribution of free dye. The dye concentration was 2.0×10^{-6} M. The excitation wavelengths were 470 and 430 nm, respectively, for DNA–AO and DNA–PF complexes. The emission wavelengths were 525 and 580 nm, respectively, for DNA–AO and DNA–PF complexes.

On the other hand, the decrease in the polarization for DNA–PF complexes is much smaller when compared to DNA–AO complexes; the polarization, in fact, remains almost constant above P/D = 20 (fig. 8). Furthermore, the anisotropy decay at P/D = 20 was almost the same as that at P/D = 200, in contrast to DNA–AO complexes which showed a marked increase of anisotropy decay with decreasing P/D ratio. Results of PF–poly d(A–T) complexes contrast with those of PF–DNA complexes. The lifetime and the quantum yield remain almost constant until conditions of incomplete binding are reached (table 1). However, the fluorescence polarization decreases with decreasing P/D ratio, in harmony with the hypothesis that energy transfer between intercalated dye molecules occurs.

Now we should recall that DNA has two types of binding sites for PF; one (AT pair) is the fluorescent site and the other (GC pair) is the quenching site [5,6,8–11]. Latt et al. [16,17] found that the lifetime and the fluorescence intensity decrease with decreasing P/D ratio when quinacrine, which behaves similarly to PF, is bound to DNA. They concluded that energy transfer between dye molecules converts dyes bound near the GC pair into energy sinks. Similar energy transfer has been postulated to account for the saturation dependence of the fluorescence intensity of DNA–acriflavine complexes [13]. Accordingly, the polarization results of PF may lead us to the idea that excitation energy is efficiently transferred from the dye bound to the fluorescent site to the dye bound to the quenching site. If this is so, such an energy transfer is not responsible for the depolarization, but causes decreases in the lifetime and the quantum yield.

With the intercalation model [57,58], the movement of PF is restricted between base pairs during the excited lifetime. Then the fluorescence decay of PF in the presence of energy transfer is predicted to have the form [22–25]:

$$I(t) = I_0 \exp[-t/\tau_0 - 2q(t/\tau_0)^{1/2}], \quad (17)$$

$$q = C/C_0, \quad (18)$$

where τ_0 is the lifetime of donor fluorescence in the absence of energy transfer, C is the molar concentration of the acceptor and C_0, the critical molar concentration of the acceptor, is given by:

$$C_0 = 3000/2\pi^{3/2} N R_0^3, \quad (19)$$

where N is Avogadro's number. If R is the average distance between intercalated dye molecules, C is assumed to be given by:

$$C = 3000/4\pi N R^3. \quad (20)$$

If dye molecules are uniformly distributed between base pairs, R is estimated by:

$$R \text{ (in Å)} = (\tfrac{1}{2} \times P/D_b + 1) \times 3.4, \quad (21)$$

where D_b denotes the concentration of bound dye. Combination of eqs. (18)–(20) leads to:

$$q = \tfrac{1}{2}\pi^{1/2}(R_0/R)^3. \quad (22)$$

Assuming appropriate values of τ_0 and q in eq. (17), several $I(t)$ functions were tested so that the numerically computed convolution with the response function of the pulse may fit the experimental curve. We usually used the lifetime at a high P/D ratio (P/D = 200) for τ_0. The solid lines in fig. 6 show the calculated best-fit curves. The fits were fairly good except for P/D = 11. The deconvoluted decay functions are listed in table 3 together with the R_0 values which were calculated according to eq. (22). The agreement between the calculated and observed decay curves at a low P/D ratio (P/D = 11) was not satisfactory; presumably due to the increased contribution of free dye to the total fluorescence. The calculated R_0 values at P/D = 15–20 are in good agreement with the theoretical value (26.4 Å). This implies that the dye binding at an intermediate P/D ratio, on the average, may result in an isotropic distribution. In this case, the average distance between two nearest intercalated molecules is about 25–35 Å. On the other hand, the R_0 value at a higher P/D ratio (P/D = 50) is much larger than the theoretical value. This is probably due to the formation of dye clusters [64]. The decay curve at P/D = 100 with denatured DNA was very similar to that at P/D = 11 with native DNA. The formation of dye clusters or the limited renatured regions of denatured DNA may result in smaller distances between two neighboring intercalated molecules and hence, more efficient energy transfer.

When the fluorescence decay is a function like eq. (17), the average value of the phase shift is expressed by a very complicated form [65]. However,

Table 3
Fluorescence lifetimes and decay functions of AO and PF bound to DNA

Dye	P/D	Free dye (%) [a]	$\langle\tau\rangle$(ns) [b]	τ(ns)		Decay function	R_0 (Å)
				c)	d)		
AO	202	0.07	5.2_5	5.5_9	5.6_4	single exponential	
(5.0×10^{-6} M)	101	0.16	5.2_5	5.6_7	5.7_1	single exponential	
	20	0.91	5.2	5.5_1	5.5_2	single exponential	
	10	2.58	5.1	5.3_8	5.3_4	single exponential	
PF	214	0.08	6.2	6.4_0	6.3_9	single exponential	
(4.8×10^{-6} M)	101	0.16	6.1	6.2_5	6.3_0	single exponential	
	51	0.35	5.7			$\exp[-t/6.4 - 0.14(t/6.4)^{1/2}]$	38
	20	1.00	4.6			$\exp[-t/6.4 - 0.80(t/6.4)^{1/2}]$	29
	11	2.71	3.6			$\exp[-t/6.4 - 1.50(t/6.4)^{1/2}]$	21
PF	204	0.04	6.2	6.6_2	6.5_7	single exponential	
(1.0×10^{-5} M)	50	0.18	5.7			$\exp[-t/6.6 - 0.16(t/6.6)^{1/2}]$	40
	20	0.51	4.6			$\exp[-t/6.6 - 0.80(t/6.6)^{1/2}]$	29
	15	0.74	4.2			$\exp[-t/6.6 - 1.40(t/6.6)^{1/2}]$	27

[a] Calculated on the basis of equilibrium dialysis [51].
[b] Determined from the phase-shift measurements.
[c] Analyzed by the method of moments [38,39].
[d] Analyzed by the Laplace transform method [40]; the time shift constants (Q values) were between 0.18 and 0.23 [40].

a decrease in the mean lifetimes ($\langle\tau\rangle$) of DNA–PF complexes with decreasing P/D ratio (fig. 2; table 3) is qualitatively explained in terms of an energy transfer mechanism [65]. The increase of the mean lifetimes below P/D = 10 (fig. 2) is ascribed to the contribution of free dye.

In conclusion, the results presented here show that energy transfer is responsible for the decay characteristics of PF bound to DNA. Bennett [41] and Mataga et al. [42] have found that dye–dye energy transfer in rigid solutions accurately satisfies the Förster decay kinetics. The DNA–PF complex is an another example. In AO–DNA, AO–polynucleotide and PF–poly d(A–T) complexes where there exists only one type of site, energy transfer causes only a depolarization of the emission. Energy transfer within the nucleic acids may be helpful for the understanding of the internal structure of the nucleic acids or the biological actions of acridine dyes. Further studies concerning energy transfer are in progress.

Acknowledgement

We thank Dr. M.S. Tung and Dr. L.H. Tang for valuable advice and helpful discussions. We also thank Miss E. Miyanohana for technical assistance.

References

[1] C.R. Cantor and T. Tao, in: Procedures in nucleic acid research, Vol. 2, eds. G.L. Cantoni and D.R. Davies (Harper and Row, New York, 1971) pp. 31–93.
[2] A.R. Peacocke, in: Acridines, 2nd Ed., ed. R.M. Acheson (Interscience, New York, 1973) pp. 723–757.
[3] E.R. Lochmann and A. Micheler, in: Physico-chemical properties of nucleic acids, Vol. 1, ed. J. Duchesne (Academic Press, New York, 1973) pp. 223–267.
[4] G. Weill and M. Calvin, Biopolymers 1 (1963) 401.
[5] Y. Kubota, Chem. Letters (1973) 299.
[6] J.P. Schreiber and M.P. Daune, J. Mol. Biol. 38 (1974) 487.
[7] B. Weisblum, Cold Spring Harbor Symposium on Quantitative Biology 83 (1974) 441.
[8] J.C. Thomes, G. Weill and M. Daune, Biopolymers 8 (1969) 647.
[9] N.F. Ellerton and I. Isenberg, Biopolymers 8 (1969) 767
[10] L.M. Chan and J.A. McCarter, Biochim. Biophys. Acta 204 (1970) 252.
[11] S. Georghiou, Photochem. Photobiol. 22 (1975) 103.
[12] R.K. Tubbs, W.E. Ditmars Jr. and Q. van Winkle, J. Mol. Biol. 9 (1964) 545.
[13] L.M. Chan and Q. van Winkle, J. Mol. Biol. 40 (1969) 491.
[14] B. Weisblum and P.L. de Haseth, Proc. Natl. Acad. Sci. US 69 (1972) 629.
[15] U. Pachmann and R. Rigler, Exp. Cell Res. 72 (1972) 602.
[16] S.A. Latt, S. Brodie and S.H. Munroe, Chromosoma 49 (1974) 17.

[17] S.A. Latt and S. Brodie, in: Excited states of biological molecule, ed. J.B. Birks (Wiley, New York, 1976) pp. 178–189.
[18] E. Fredericq and C. Houssier, Biopolymers 11 (1972) 2281.
[19] A. Orgel and S. Brenner, J. Mol. Biol. 3 (1961) 762.
[20] A. Albert, The acridines, 2nd Ed. (Arnold, London, 1966) pp. 493–503.
[21] Y. Kubota, Chem. Letters (1977) 311.
[22] Th. Förster, Ann. Physik 2 (1948) 55.
[23] Th. Förster, Z. Naturforsch. 4a (1949) 321.
[24] M.D. Galanin, Soviet Phys. JETP 1 (1955) 317.
[25] Th. Förster, in: Modern quantum chemistry, ed. O. Sinanoglu (Academic Press, New York, 1965) pp. 93–137.
[26] Y. Kubota and Y. Fujisaki, Bull. Chem. Soc. Japan, 50 (1977) 297.
[27] H.R. Mahler, B. Kline and B.D. Mehrotra, J. Mol. Biol. 9 (1964) 801.
[28] R.B. Inman and R.L. Baldwin, J. Mol. Biol. 8 (1964) 452.
[29] C.A. Parker and W.T. Rees, Analyst 85 (1960) 587.
[30] W.H. Helhuish, J. Phys. Chem. 65 (1961) 229.
[31] J.N. Demas and G.A. Crosby, J. Phys. Chem. 75 (1971) 991.
[32] M. Almgren, Photochem. Photobiol. 8 (1968) 231.
[33] M. Shinitzky, J. Chem. Phys. 56 (1972) 5979.
[34] E.D. Cehelnik, K.D. Mielenz and R.A. Velapoldi, J. Res. Natl. Bur. Std. US A79 (1975) 1.
[35] K.D. Mielenz, E.D. Cehelnik and L. McKenzie, J. Chem. Phys. 64 (1976) 360.
[36] T. Azumi and S.P. McGlynn, J. Chem. Phys. 37 (1962) 2413.
[37] J.B. Birks, Photophysics of aromatic molecules (Wiley–Interscience, New York, 1970) pp. 94–97.
[38] I. Isenberg and R.D. Dyson, Biophys. J. 9 (1969) 1337.
[39] I. Isenberg, R.D. Dyson and R. Hanson, Biophys. J. 13 (1973) 1090.
[40] A. Gafni, R.L. Modlin and L. Brand, Biophys. J. 15 (1975) 263.
[41] R.G. Bennett, J. Chem. Phys. 41 (1964) 3037.
[42] N. Mataga, H. Obashi and T. Okada, J. Phys. Chem. 73 (1969) 370.
[43] T.L. Nemzek and W.R. Ware, J. Chem. Phys. 62 (1975) 477.
[44] A.E.W. Knight and B.K. Selinger, Spectrochim. Acta A27 (1971) 1223.
[45] A. Jablonski, Bull. Acad. Polon. Sci. Ser. Math. Astron. Phys. 8 (1960) 259.
[46] R.D. Spencer and G. Weber, J. Chem. Phys. 52 (1970) 1654.
[47] G. Löber, Photochem. Photobiol. 4 (1965) 607.
[48] S. Yamabe, Arch. Biochem. Biophys. 130 (1969) 148.
[49] R.D. Spencer and G. Weber, Ann. NY Acad. Sci. 158 (1969) 361.
[50] T.G. Scott, R.D. Spencer, N.J. Leonard and G. Weber, J. Am. Chem. Soc. 92 (1970) 687.
[51] Y. Kubota, Y. Eguchi, K. Hashimoto, M. Wakita, Y. Honda and Y. Fujisaki, Bull. Chem. Soc. Japan 49 (1976) 2424.
[52] R.W. Armstrong, Y. Kurucsev and U.P. Strauss, J. Am. Chem. Soc. 92 (1970) 3174.
[53] D.F. Bradley and M.K. Wolf, Proc. Natl. Acad. Sci. US 45 (1959) 944.
[54] A.L. Stone and D.F. Bradley, J. Am. Chem. Soc. 83 (1961) 3627.
[55] J.W. MacInnes and M. McClintock, Biopolymers 9 (1970) 1407.
[56] M. Gilbert and P. Claverie, in: Molecular associations in biology, ed. B. Pullman (Academic Press, New York, 1968) pp. 245–260.
[57] L.S. Lerman, J. Mol. Biol. 3 (1961) 18.
[58] L.S. Lerman, Proc. Natl. Acad. Sci. US 49 (1963) 94.
[59] K. Beardsley and C.R. Cantor, Proc. Natl. Acad. Sci. US 65 (1970) 39.
[60] R.E. Harrington, J. Am. Chem. Soc. 92 (1970) 6957.
[61] R.S. Knox, Physica 39 (1968) 361.
[62] J. Paoletti and J.B. LePecq, J. Mol. Biol. 59 (1971) 43.
[63] D. Genest, Ph. Wahl and H.C. Auchet, Biophys. Chem. 1 (1974) 266.
[64] R.F. Steiner, I. Weinryb and R. Kolinski, Biochim. Biophys. Acta 209 (1970) 306.
[65] S. Georghiou, J. Phys. B 2 (1969) 1084.